

## Two-Phase Shear Band Structures at Uniform Stress

Melanie M. Britton and Paul T. Callaghan

*Department of Physics, Massey University, Palmerston North, New Zealand*  
(Received 13 December 1996; revised manuscript received 26 March 1997)

Using NMR microscopy we measure the velocity distribution for a wormlike surfactant solution in the gap of a small angle cone-and-plate rheometer. This system, cetylpyridinium chloride/sodium salicylate 100 mM/60 mM, exhibits biphasic shear band structure when the applied shear rate exceeds the critical rate of strain beyond which a plateau is observed in the shear stress. The structure is characterized by two low/high shear interfaces and the region of high shear evolves by increasing width as the average gap shear is increased. [S0031-9007(97)03449-2]

PACS numbers: 47.54.+r, 07.10.Pz, 47.17.+e

One very interesting nonlinear constitutive property of some complex fluids concerns nonmonotonic behavior in the stress vs strain rate curve (the flow curve) and the flow characteristics of such fluids have been the subject of considerable theoretical conjecture [1–5]. The class of viscoelastic fluid for which the flow curve exhibits a stress minimum, as shown schematically in Fig. 1, includes both high molecular weight polymeric liquids [6] and solutions of wormlike surfactant [7]. In these latter fluids, amphiphilic surfactant molecules aggregate reversibly into long, flexible, cylindrical structures which overlap and form an entangled network in which the relaxation process is determined by a combination of reptation and breaking processes. The effect of the rapid breakage/formation process is to preaverage any variation in the reptation time associated with polydispersity effects so that the characteristic relaxation time  $\tau$  is sharply defined, yielding a near-Maxwell behavior in the linear response. In the nonlinear flow curve, the stress first rises and then falls with increasing shear rate, the critical shear rate which defines the maximum in the stress being [8]  $\dot{\gamma}_c = 2.6/\tau$ . The region of decreasing stress as the shear rate increases finds its origin in the reduction in entanglements as the worm chains align in the flow. This section of the flow curve is associated with unstable flow [4].

At much higher shear rates, the more rapid dynamics associated with the local motion of the micelles and the viscosity of the solvent are expected to cause an upturn in the flow curve. Cates *et al.* [2] have suggested that because of the instability beyond the shear rate corresponding to the stress maximum  $\sigma_c$  in the schematic flow curve, separation of distinct shear bands may occur, in the manner of a first order phase separation. These bands will be associated with the intersections of a stress tie line with the upper and lower branches of the underlying flow curve and the proportions of each band will be as required to satisfy the average shear rate. The precise structure of such shear bands is a delicate problem about which the various theoretical treatments produce uncertain results and in support of which no clear experimental tests are available, especially under ideal conditions of uniform stress.

The velocity profile expected for a fluid exhibiting an inflected intrinsic flow curve has previously been the subject of considerable speculation for commonly encountered geometries where the shear stress varies strongly through the fluid, such as in pipe or cylindrical Couette flow. For example, the instability associated with the inflection is expected to lead to the “spurt effect” in pipes [1] and to generate shear bands in a Couette cell [2,9]. Indeed some evidence for the existence of such cylindrical Couette shear banding has been found using optical and nuclear magnetic resonance (NMR) microscopy methods [10,11]. However, in neither of these experiments were details of the band structure apparent and, in the case of the NMR data, the high shear rate band was confined to a single pixel. In a sense, the shear inhomogeneity which is present in the cylindrical Couette experiment complicates any modeling of shear banding effects. Hence an ideal test for theoretical predictions [3,4] is one in which uniform stress conditions exist.

In this Letter we report on a direct NMR microscopy measurement of shear banding effects in the wormlike surfactant system cetylpyridinium chloride/sodium salicylate in aqueous solution at 100 mM/60 mM concentration [12]. In order to obtain conditions of near-uniform stress we place the fluid in the gap of a small angle cone-and-plate rheometer, i.e., between the flat lower plate and

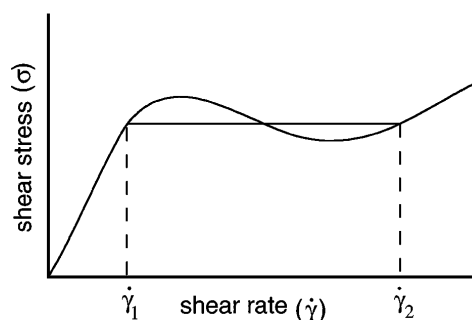


FIG. 1. Schematic flow curve for a fluid exhibiting double-valued stress vs rate-of-strain behavior. In the phase separation model for shear banding [2],  $\dot{\gamma}_1$  and  $\dot{\gamma}_2$  correspond to coexisting shear rates at a single stress value.

an upper conical surface whose vertex just contacts that plate. By rotating the cone at constant angular velocity the fluid is subject to a shearing action in which, to first order, the local stress  $\sigma(\theta)$  is independent of radius and varies with polar angle as  $\sigma(\theta) = \sigma(90^\circ)\text{cosec}^2\theta$  [13]. For a typical gap angle of  $4^\circ$  this corresponds to a variation across the gap of less than 0.5%. Given a fluid in which the stress has a single-valued dependence on rate of strain  $\dot{\gamma}$ , the shear rate across the gap is expected to be correspondingly uniform and given by  $\omega/\tan\alpha$ , where  $\omega$  is the angular speed of the cone and  $\alpha$  is the gap angle. Measurements of the cone torque at any applied strain rate provide the viscometric data which characterizes the constitutive behavior of a fluid in terms of the shear rate-dependent stress  $\sigma(\dot{\gamma})$ . It should be noted that the wormlike surfactant system of present interest exhibits, in the cone-and-plate system, a critical rate of strain  $\dot{\gamma}_c$ , on the order of  $1\text{ s}^{-1}$ , beyond which a wide range of shear rates is found to be consistent with a plateau (at round 25 Pa) in the applied stress [8,12,14]. Such a plateau is believed to be consistent with the formation of separated high and low shear rate phases within the gap.

Our cone-and-plate rheometers comprise shearing surfaces made of the machinable glass, MACOR (Corning, New York) with cone angles of  $4^\circ$  and  $7^\circ$ . These cells are mounted inside the 25 mm resonator of an NMR probe system comprising a three axis gradient coil assembly. This probe is located inside the bore of a 7 T superconducting magnet and a rod connects the cone shaft to a stepping motor and gearbox mounted above the top of the magnet bore. The sample is maintained at a temperature of  $25^\circ$  by a controlled airstream. NMR imaging experiments were carried out using the proton NMR signal at 300 MHz.

The motion-sensitive NMR microscopy method which we use has been described in detail elsewhere [15]. By appropriate manipulation of magnetic field gradient pulses and resonant radiofrequency pulses we are able to independently phase encode the NMR signal both for nuclear spin position as well as for translational displacement over a fixed time interval, on the order of 20 ms. Our reconstruction method uses a Fourier analysis in order to directly compute the local velocity distribution for each pixel of the spatially resolved image. The technique has been extensively tested in a wide class of measurements and has shown itself to be sensitive and robust, allowing velocity resolution on the order of  $10\text{ }\mu\text{m s}^{-1}$  at a spatial resolution of around  $(20\text{ }\mu\text{m})^2$ . In our method a 2 mm thick planar slice of spins is excited normal to the velocity-encoding direction, and a two-dimensional image of that plane is obtained. By using a magnetic field gradient which is larger in the vertical direction than in the horizontal direction, we are able to show an expanded gap region. With this expanded vertical scale the pixel resolution is  $36\text{ }\mu\text{m}$  in the vertical direction and  $215\text{ }\mu\text{m}$  horizontally. It should be noted that the proton NMR signal is chemically

nonselective and arises predominantly from the spins in the solvent water molecules. We have carried out extensive measurements of the velocity distribution in our cone-and-plate gaps using both Newtonian fluids (water and glycerol) and a shear-thinning non-Newtonian fluid [an 11.5 g/dL solution of 0.6 million dalton polystyrene in decalin] and find that the velocity gradient is very uniform, in complete agreement with the constant rate-of-strain assumption.

For the wormlike surfactant system, the velocity gradients show no deviation from linearity at very low shear rates while for apparent shear rates clearly in excess of  $\dot{\gamma}_c$  we consistently observe a dramatic variation in the rate of strain across the gap. Figure 2(a) shows a grey scale image of the vertical derivative of the velocity in the  $4^\circ$  cone gap at  $\dot{\gamma}_{\text{app}} = 16\text{ s}^{-1}$ . A very high shear rate band exists at midgap (i.e., fixed angle  $\theta \approx 90^\circ - \alpha/2$ ) and independent of radius. We have repeated these experiments using the  $7^\circ$  cone and plate system and have seen identical behavior.

Of particular interest is the development of the shear band structure across a wide range of shear rates. Above a rate of strain of around  $20\text{ s}^{-1}$ , and for the prolonged period ( $\approx 2\text{ h}$ ) needed for the NMR measurement, fluid is

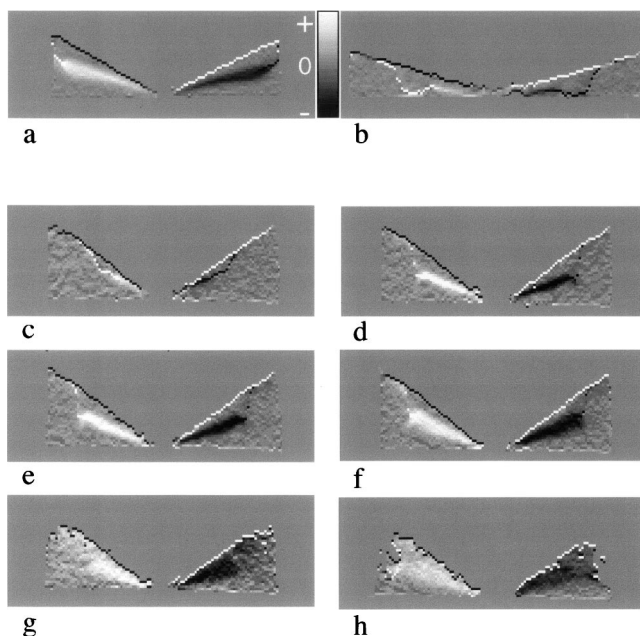


FIG. 2. Shear rate images for cetylpyridinium chloride/NaSal wormlike surfactant solution. The horizontal field of view is 28 mm. The grey scale indicates the shear rate in arbitrary units. Note the opposite sign shear for the receding and advancing segments of fluid on opposite sides of the gap. (a) In a  $4^\circ$  gap (vertical gain  $\times 6$ ) with free exterior fluid surface and at an apparent shear rate,  $\omega/\tan\alpha$ , of  $16\text{ s}^{-1}$ . (b) In a  $7^\circ$  gap (vertical gain  $\times 3$ ) with outer containment jacket and at a lower shear rate of  $7\text{ s}^{-1}$ . (c)–(h) show further shear rate images for a  $7^\circ$  gap (vertical gain  $\times 6$ ) covering the range (c)  $7\text{ s}^{-1}$ , (d)  $11\text{ s}^{-1}$ , (e)  $14\text{ s}^{-1}$ , (f)  $19\text{ s}^{-1}$ , (g)  $36\text{ s}^{-1}$ , and (h)  $48\text{ s}^{-1}$ .

expelled from the gap, presumably due to the action of the normal forces associated with elastic behavior. In order to avoid this problem we have carried out experiments using a  $7^\circ$  cone-and-plate system in which the outer surface of the gap fluid, rather than being in contact with air and therefore free to rotate, contacts a containment jacket made of Teflon, this material being chosen to minimize drag. The images of Figs. 2(c)–2(h) show a progression with apparent shear rates ranging from 7 to  $48 \text{ s}^{-1}$ , i.e., from just above the critical shear rate to a region well out in the apparent stress plateau. A remarkable evolution in band structure is apparent. At the lowest shear rate the band is located within the gap center at small radii, but wanders with increasing radial displacement to contact both the upper and lower surfaces, an effect which is particularly apparent in another experiment shown in Fig. 2(b). Beyond this shear rate the band is clearly located at midgap and at an angle which is independent of radius, out to a critical radial displacement where shear banding effects vanish, presumably due to perturbations from the outer containment wall. We shall be concerned to understand the band structure well away from the wall perturbation region.

In Fig. 3(a) we show a series of profiles across the gap taken from the data shown in Figs. 2(c)–2(h). In these data several clear features emerge. First, three bands are present, the central high shear band having two interfaces to adjacent low shear regions. Second, the symmetry of the midgap location of the high shear rate band is remarkable and apparent in all our experiments, including some where the cone-and-plate alignment is imperfect.

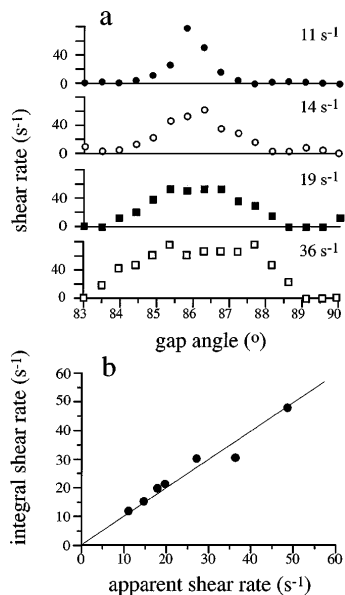


FIG. 3. (a) Measured shear rate profiles along a line of approximately fixed radius of 4.4 mm from core apex for the  $7^\circ$  cone-and-plate data of Fig. 2, for 11, 14, 19, and  $36 \text{ s}^{-1}$ . (b) Mean integral shear rate (calculated by summing across the bands shown in Fig. 2) vs apparent shear rate  $\dot{\gamma}_{\text{app}} = \omega / \tan \alpha$ .

Third, we note that as the cone rotation speed and, hence, the gap apparent shear rate, is increased, the high shear rate band expands in width at approximately a constant maximum shear rate (around  $60 \text{ s}^{-1}$ ). Fourth, we observe that the central high shear band has an interface with the adjacent low shear regions, of characteristic thickness around  $1.5^\circ$  (but with half this width in the  $4^\circ$  gap rheometer) and that this interfacial angular thickness remains constant over a wide range of shear rates and central bandwidths. Fifth, we note that the sharpness of the observed velocity distributions in each pixel implies that the measured shear rate profiles are highly stable. Finally, in confirmation of our measurement accuracy, we show in Fig. 3(b) the good agreement between integrated mean of the shear profile vs the mean apparent shear rate  $\omega / \tan \alpha$ .

The geometrical distribution and structure of shear bands for fluids exhibiting inflected flow curves is a matter of conjecture. In particular, several authors have predicted [3–5] that there exists only one stress (the coexistence stress) at which stable banded flow is possible. Such a prediction determines that the higher shear rate band should exhibit a unique rate of strain, corresponding to the intersection of the coexistence stress with the upper branch of the flow curve, and that with increasing gap shear the high shear band will grow in width but not in shear rate amplitude, in a manner akin to a first order phase transition. This is precisely our observation, and, to our knowledge, the first report of such a phenomenon. The results reported here lend credence to the concept of a coexistence stress. Furthermore, the value of the observed upper branch rate of strain agrees well with the value at which a deviation from plateau stress is found in the rheometric data [12,14] and is close to that predicted by Spenley *et al.* [3].

However, the matter of the spatial distribution of the two phases is not at all clear in the various theoretical treatments for near-uniform stress. In the calculations of Spenley *et al.* the position is indeterminate, while those of Espanol *et al.* [4] exhibit a simple two band structure with the high shear rate band adjacent to one wall. Greco and Ball [5], however, calculate that a three band structure can evolve for cylindrical Couette flow in an exceptionally narrow gap whose stress variation is around 2%. This prediction is particularly interesting in light of the weak stress variation of around 0.5% and 1.5%, respectively, for the  $4^\circ$  and  $7^\circ$  cone-and-plate gaps. However, the central location of our high shear rate band, independent of gap angle, is a dramatic feature for which no clear explanation emerges. We note, for example, that for all realistic values of the fluid viscoelastic parameters,  $\sigma(r, \theta)$  is characterized by a radially independent, monotonic variation with angle  $\theta$  from cone to plate with no indication of a stress maximum (or a stress minimum) at the midgap angle [13]. If secondary flow were present then there could exist

a circulation pattern involving components of velocity within the image plane [13]. Secondary flow streamlines tend to be concentrated near the cone-and-plate surfaces so that the vicinity of the midgap angle represents a near stagnant region. However, we do not expect significant secondary flow at the small gap angle used here, this null result being confirmed in a separate experiment in which we encode for velocity within the plane.

One other feature of note in the present experiments concerns the thickness of the interfacial region. The matter of interface width has been addressed by Spenley, Yuan, and Cates [3] who postulated that it could be determined by the gradient in the viscoelastic contribution ( $\sigma_e$ ) to the total stress so that the constitutive equation contains an additional interfacial term,  $-\gamma \partial^2 \sigma_e / \partial y^2 \cdot \gamma$  has the dimensions of a diffusion coefficient and the interface thickness is predicted to be  $(\gamma \tau)^{1/2}$ . Our measurements at the  $7^\circ$  gap angle suggest a value for  $\gamma$  (expressed as an angular diffusion coefficient) of  $3 \times 10^{-4} \text{ rad}^2 \text{ s}^{-1}$ , with a value of around  $1 \times 10^{-4} \text{ rad}^2 \text{ s}^{-1}$  at a  $4^\circ$  gap, a difference which suggests that interfacial properties are strongly influenced by stress uniformity.

The existence of an interface of finite thickness raises important questions concerning how the fluid can maintain a distinct high shear rate band when  $\dot{\gamma}_{\text{app}}$  is closer to  $\dot{\gamma}_c$ . In particular, if the shear rate maximum is required to lie on the line of coexistence stress (i.e.,  $\dot{\gamma} \approx 60 \text{ s}^{-1}$ ), then the band structure shown in Fig. 3(a) and corresponding to  $\dot{\gamma}_{\text{app}} = 11 \text{ s}^{-1}$ , represents the lowest shear rate structure consistent with the interface requirement. We suggest that the migration of the band to the rheometer surface at shear rates below  $7 \text{ s}^{-1}$  represents an attempt by the fluid to satisfy the coexistence stress requirement without the need for the finite interface width associated with a high shear rate band located in the bulk of the fluid.

The wormlike micelle system has provided a model for the demonstration of shear banding effects. That such distinctive banding occurs under conditions of near-uniform stress provides a graphic illustration of the underlying subtlety of the fluid dynamics. It also provides a nice test for hydrodynamic theories which incorporate the intrinsic

constitutive properties of the fluid. The remarkable band symmetry which we observe suggests that the cone-and-plate geometry has some distinct advantages as a platform on which to develop theoretical predictions.

The authors are grateful to Professor M. E. Cates and Dr. N. A. Spenley for helpful advice and to Dr. F. Greco and Dr. R. C. Ball for providing us with a preprint of their work. We also acknowledge financial support from the New Zealand Foundation for Research, Science and Technology.

- 
- [1] T. C. B. McLeish and R. C. Ball, *J. Polym. Sci.* **24**, 1735 (1986).
  - [2] M. E. Cates, T. C. B. McLeish, and G. Marrucci, *Europhys. Lett.* **21**, 451 (1993).
  - [3] N. A. Spenley, X. F. Yuan, and M. E. Cates, *J. Phys. II (France)* **6**, 551 (1996).
  - [4] P. Espanol, X. F. Yuan, and R. C. Ball, *J. Non-Newton. Fluid Mech.* **65**, 93 (1996).
  - [5] F. Greco and R. C. Ball, *J. Non-Newton. Fluid Mech.* (to be published).
  - [6] M. Doi and S. F. Edwards, *The Theory of Polymer Dynamics* (Oxford University Press, Oxford, 1987).
  - [7] M. E. Cates and S. J. Candau, *J. Phys. Condens. Matter* **2**, 6869 (1990).
  - [8] M. E. Cates, *J. Phys. Chem.* **94**, 371–375 (1990), and references therein.
  - [9] N. A. Spenley, M. E. Cates, and T. C. B. McLeish, *Phys. Rev. Lett.* **71**, 939 (1993).
  - [10] R. Makhloufi, J. P. Decruppe, A. Ait-Ali, and R. Cressely, *Europhys. Lett.* **32**, 253 (1995).
  - [11] R. W. Mair and P. T. Callaghan, *Europhys. Lett.* **36**, 719 (1996).
  - [12] H. Rehage and H. Hoffman, *Mol. Phys.* **74**, 933 (1991).
  - [13] K. Walters and N. D. Waters, *Polymer Systems: Deformation and Flow* (Macmillan, London, 1968), p. 211.
  - [14] P. T. Callaghan, M. E. Cates, C. J. Rofe, and J. B. A. F. Smeulders, *J. Phys. II (France)* **6**, 375 (1996).
  - [15] P. T. Callaghan, *Principles of Nuclear Magnetic Resonance Microscopy* (Oxford University Press, New York, 1991).